Does a Finer Level of Detail of a 3D City Model Bring an Improvement for Estimating Shadows?

Filip Biljecki, Hugo Ledoux and Jantien Stoter

Abstract 3D city models are characterised by the level of detail (LOD), which indicates their spatio-semantic complexity. Modelling data in finer LODs results in visually appealing models and opens the door for more applications, but that is at the expense of increased costs of acquisition, and larger storage footprint. In this paper we investigate whether the improvement in the LOD of a 3D building model brings more accurate shadow predictions. The result is that in most cases the improvement is negligible. Hence, the higher cost of acquiring 3D models in finer LODs is not always justified. However, the exact performance is influenced by the architecture of a building. The paper also describes challenges in experiments such as this one. For instance, defining error metrics may not always be simple, and the big picture of errors should be considered, as the impact of errors ultimately depends on the intended use case. For example, an error of a certain magnitude in estimating the shadow may not significantly affect visualisation purposes, but the same error may considerably influence the estimation of the photovoltaic potential.

1 Introduction

Level of detail (LOD) is a fundamental concept in GIS and 3D city modelling: it indicates the data set's resolution, usability, and the degree of abstraction of reality (Biljecki et al. 2014b). The concept is borrowed from computer graphics, where

F. Biljecki (✉) · H. Ledoux · J. Stoter
3D Geoinformation, Delft University of Technology, Delft, The Netherlands
e-mail: f.biljecki@tudelft.nl

H. Ledoux
e-mail: h.ledoux@tudelft.nl

J. Stoter
e-mail: j.e.stoter@tudelft.nl

A. Abdul-Rahman (ed.), *Advances in 3D Geoinformation*,
Lecture Notes in Geoinformation and Cartography,
DOI 10.1007/978-3-319-25691-7_2

Fig. 1 Our research in a nutshell: the estimation of the shadow differs between the different levels of detail, and the accuracy of the prediction seems to increase with each LOD. However, this should be investigated numerically and it is not straightforward as it may appear

it is used to balance the computational complexity and the visualisation quality (fidelity). The latter, i.e. how similar the object looks like to the original one, can be assessed with error metrics such the deviation between the geometry of the original model and the geometry of its simplified counterpart (Luebke et al. 2003).

Such rationale can be applied to geoinformation science, in order to analyse whether it is worth to invest funds and computational resources in data set of a particular LOD. However, in 3D GIS, models are often used beyond visualisation for several purposes which significantly differ from each other—they have different behaviour, different requirements for LODs, and an outcome of different nature. For instance, 3D city models are used to estimate the real estate net internal area in m^2 (Boeters et al. 2015), insolation of buildings in kWh/year (Biljecki et al. 2015a), and noise in dB (Stoter et al. 2008), resulting in different kinds of errors, differently influenced by a particular LOD.

The aim of this paper is to investigate the influence of the resolution of spatial data on the quality of a particular spatial analysis: the estimation of shadows in an urban environment (Fig. 1). This use case is frequent in 3D GIS, and it is used in several application domains, for instance to assess the shadow impact of new buildings to their surroundings (Sect. 2).

For a number of LODs, we compute their errors when used for this purpose. However, conducting such analysis is burdened by difficulties, among others: (1) multi-LOD data sets are seldom available hindering such studies (Biljecki et al. 2015b); (2) available multi-LOD data sets normally contain real-world acquisition errors, inhibiting the comparison between LODs, since it is hard to isolate the error induced by the degree of abstraction from the error caused by the acquisition; (3) the outcome of each spatial analysis may not be unambiguously quantifiable, so the accuracy cannot be easily expressed (Biljecki et al. 2015c); and (4) from the implementation aspect, it is not always easy to automatically run a spatial operation for a large data set and extract results in a format that is suitable for error analysis. We mitigate these problems with an approach supported by a procedural modelling engine to automatically construct CityGML models in multiple LODs (Sect. 3). The results (Sect. 4) are relevant for practitioners because they can aid them to decide whether it is worth to acquire buildings in finer LODs considering that they come with an increased cost of acquisition and storage.

2 Related Work and Background

2.1 *Influence of Data Granularity on Spatial Analysis*

Studies on the influence of the scale, LOD, and resolution to the quality of a GIS operation are focused on 2D and to raster representations. Hengl (2006) discusses the importance of considering the resolution of a raster, and underlines that in GIS projects the resolution is usually selected without any scientific justification. Usery et al. (2004) determined the resolution effects on watershed modelling by resampling input rasters, and concluded that the resolution has a significant effect on the accuracy of the result. Booij (2005), Chaubey et al. (2005), Ling et al. (2008), and Pogson and Smith (2015) performed similar analyses with similar results.

In 3D GIS such studies are rare. A possible reason is that 3D city models cannot be simply "resampled" to easily obtain additional LODs for analysis.

Brasebin et al. (2012) tested the fitness for use of LOD1 and LOD2 models of two French data sets in the determination of the sky view factor (SVF). The result is that for 75 % of the analysed samples the improvement in accuracy is less than 2 %. Besuievsky et al. (2014) carry out a similar study with SVF focusing on the windows of buildings, with a few variants of high-detailed architectural models, and find a significant difference in the results.

Strzalka et al. (2011) investigate the use of 3D city models for forecasting energy demand, and argue that the suitability of an LOD depends on the configuration of buildings (i.e. for an area with predominantly flat roofs they suggest that an LOD1 suffices). However, experiments with other LODs are not documented.

Kibria et al. (2009) survey the perceptual value of a few LODs in spatial planning. It turns out that in some planning phases a finer LOD is actually undesirable.

2.2 *The Role of Shadow in GIS*

The estimation of shadows cast by buildings is a common topic in geoinformation science, and it is important for a number of application domains, such as thermal comfort (Hwang et al. 2011; Yezioro and Shaviv 1994) and solar energy (Carneiro and Golay 2009; Strzalka et al. 2012). This use case may be related to the visibility operation which is used for diverse purposes (Bartie et al. 2010; Peters et al. 2015). In this context, the estimation of shadow is a variation of the visibility problem, with the particularity that the sun is practically an infinitely distant point resulting in parallel rays, and that its position is variable.

Herbert and Chen (2015) underline that understanding shadow is crucial in urban planning, for assessing the effect new buildings induce on existing ones. They perform a survey among urban planners on the quality of the visualisation of the shadow based on different visual representations (e.g. level of transparency, 2D vs. 3D), and also include a query about the suitability of the LOD. However, only LOD1 was given as an option, and the participants were given the opportunity to perceptually assess whether a 3D model of LOD1 is sufficient or not for such analysis.

Estimating shadows is important for determining solar envelopes, the subset of urban space with a certain period of assured access to sunshine (Knowles 2003). These are defined in terms of discrete numbers of hours of sun, but they can also be defined in terms of solar irradiation (Morello and Ratti 2009). Solar envelopes are to a degree enshrined in local and state laws, where residents are protected with the right to solar access (e.g. the façade of houses must receive a certain amount of hours of direct sunlight per day; see Den Haag 2011 and City of Mississauga 2012 for exemplary regulations).

In urban planning, shadows are not analysed only for buildings, for instance, Lange and Hehl-Lange (2005) study shadow casting from a proposed wind turbine, and Kumar et al. (1997) forecast occlusion by terrain.

Accounting for shadows is common when estimating the solar potential of buildings (Mardaljevic and Rylatt 2003; Carneiro and Golay 2009; Tooke et al. 2011; Redweik et al. 2013; Eicker et al. 2015; Nguyen and Pearce 2012; Hofierka and Zlocha 2012). Strzalka et al. (2012) develop a method to determine the shadow projected on a roof surface in order to account for the reduced yield of solar panels when estimating the feasibility of their installation. The method is designed as a visibility problem between small triangular partitions of a surface and the sun at various timestamps. The centroid of each partition is tested for visibility to the sun, and if the sun's ray intersects any of the other surfaces, the partition is marked as shaded at that timestamp.

In a related research, Alam et al. (2013) note that while LOD1 block models are sufficient for shading, higher LODs will inherently bring different results. However, this is not supported empirically, and in this paper we bridge this gap.

Jochem et al. (2009) develop a method for estimating the insolation of roofs from point clouds, taking into account shadows. While they deal with a single-LOD representation, they highlight that roof overhangs and chimneys may play an important factor in the magnitude of the shadow. This is important, because different LODs contain a different degree of detail, and in our research we investigate their claim.

Shadowing plays an important role in the research of Helbich et al. (2013). Their premise is that solar radiation is significantly capitalised in flat prices, and they consider the shadow effect in order to improve the accuracy of a hedonic house price model. They highlight that such simulations should be conducted for different positions of the sun because of the considerable differences in the results.

Finally, shadows are crucial in geo-visualisation to increase the quality of the visual communication (Appleton and Lovett 2003).

2.3 *The Role of Shadow in Computer Graphics*

Shadows have a longstanding underpinning in computer graphics where they play a significant role, as they enhance the realism of the scene and provide cues of spatial relations such as depth (Williams 1978; Woo et al. 1990). As a result, many algorithms have been developed to estimate shadows and enhance realism, e.g. recursive ray tracing (Whitted 1980). Furthermore, many other computer graphics algorithms are closely related to this topic and frequently applied, e.g. the determination of shaded portion of the roof when estimating the insolation may be considered as a ray-triangle intersection problem (Möller and Trumbore 1997). We consider such algorithms in the design of our experiment.

3 Methodology

Our methodology for estimating whether finer LODs bring improvements in the estimation of shadows consists of the following stages:

1. Producing multi-LOD data: procedural generation of 3D city models (in CityGML).
2. Shadowing: rendering shadows from the models, and obtaining the shadow in a GIS form for analysis. We consider the shadow a building casts on the ground.
3. Analysis: quantification of shadows, and measuring their error for each LOD.

3.1 Source of Data and Considered LODs

In our approach, as a source of multi-LOD data we use procedurally modelled 3D models stored in CityGML in multiple LODs. The models have been generated by Random3Dcity, an open-source project of Biljecki et al. (2014a). The advantage of procedurally generated data is that they are not burdened by acquisition errors, and that a large number of 3D models can be obtained easily. Synthetic data have been previously diversely used in GIS (see, among others, Li et al. 2000 and Burnicki et al. 2007).

In principle, for our tests we use the traditional CityGML LODs (Gröger and Plümer 2012). However, the engine generates multi-LOD data based on a specification of Biljecki et al. (2016), which refines these LODs, providing us with a larger number of representations to benchmark. We use the following representations. LOD1.1 is a block model obtained with extrusion to a single height, LOD1.2 mandates smaller building parts (e.g. alcoves), and in LOD1.3 each building part has its own height (a building does not have a single height as in 1.1/1.2). LOD2.0 is similar to 1.1, with the addition of a simple roof structure. LOD2.1 adds smaller building parts, and LOD2.2 requires dormers and other roof superstructures of similar size. LOD2.3 demands the explicit modelling of roof overhangs (such models are usually constructed in a combination of terrestrial and airborne techniques). LOD3, the finest LOD, contains openings, roof overhangs, and smaller façade details. Because

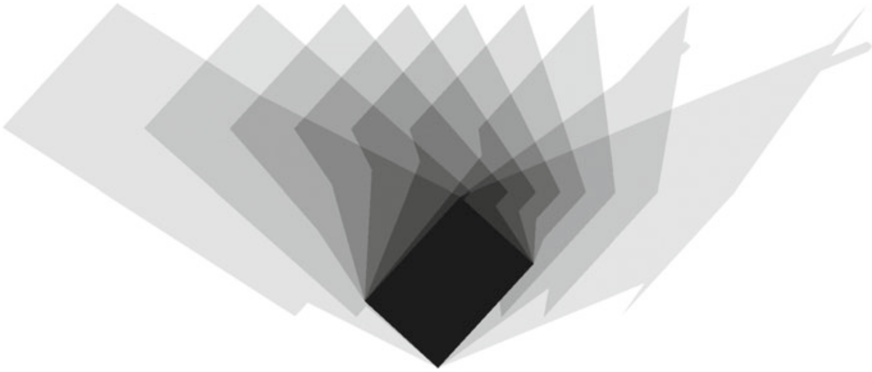

Fig. 2 Orthogonal *top view* composite of 9 shadows during a day (also known as the butterfly shadow diagram; the *outline* of each shadow is drawn at hourly intervals) for an LOD3 model. It suggests the different degree of influence of LOD-related details on the shadow depending on the date, time, and location. The building footprint is shown in *black*

this is the finest representation available, we consider it as ground truth. Figure 1 shows the following LODs: 1.1, 2.0, 2.1, and 3.

3.2 Sun Position and Location on Earth

Figure 2 indicates a substantial difference in the behaviour of this spatial analysis when it comes to the different relative position of the sun, caused by the different time of day and location on Earth. In order to diversify our experiments, we consider two locations: Delft (Netherlands) and Kuala Lumpur (Malaysia), and several timestamps during three characteristic days in 2015: spring equinox (20 March), summer solstice (21 June), winter solstice (22 December), and an arbitrary day: 27 April. This variety results in 81 different positions of the sun spread over daytime.

3.3 Computation of the Shadow

We define the shadow S^{B_i} as the subset of the $\mathbb{R}^2$ (the ground, a horizontal plane in our case, considered as the shadow receiver) that is occluded by a building B_i. When 3D city models are utilised $S_r^{B_i}$ denotes the shadow forecast with a data set of the representation (LOD) r. We compute the shadow by projecting each polygon of a building model B_i to the plane with a perspective transformation (Blinn 1988), according to the position of the sun. The union of the projected polygons represents the shadow (Fig. 3), however, in the final step we adjust the polygon by removing the footprint of B_i.

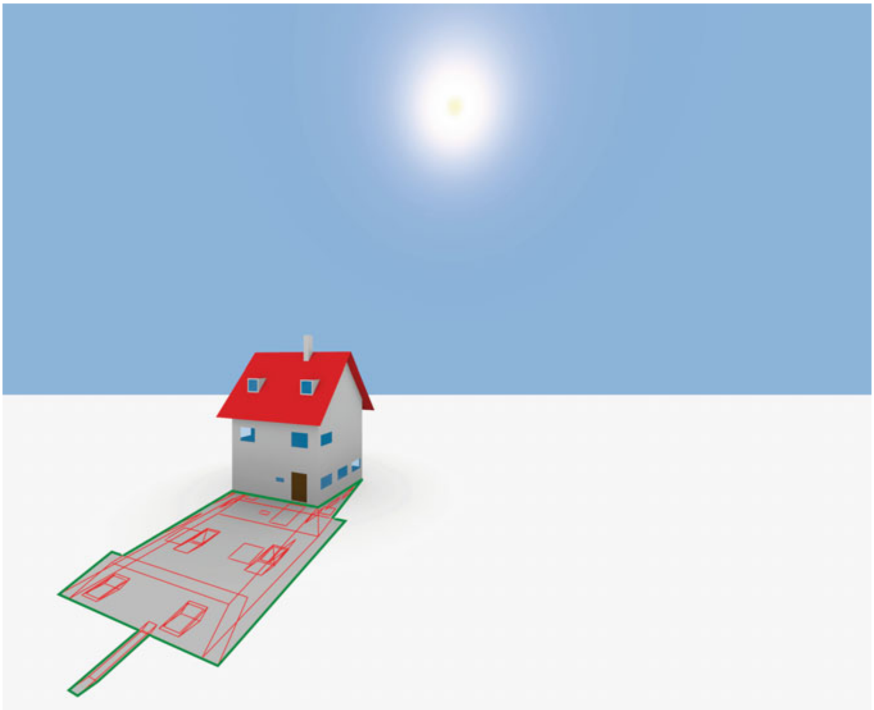

Fig. 3 In our approach and our software implementation, the shadow on the ground is derived as a unionised set (*green*) of projected polygons (in *red*; 51 polygons in this LOD3 case) from the CityGML model, and accounting for the footprint

3.4 Selection of Error Metrics

The shadow cast on the ground is a polygon, thus the first measure that comes to mind to quantify a shadow is its area $a(S^{B_i})$, and to compare it to the ground truth:

$$\varepsilon_1^r = a(S_r^{B_i}) - a(S^{B_i})$$

However, the deviation of the estimated value is inconclusive, as it appears in Fig. 4. Therefore we introduce a new metric: the area of the symmetric difference (the union without the intersection—see the light red area in the same figure):

$$\varepsilon_2^r = a(S_r^{B_i} \ominus S^{B_i}) = a((S_r^{B_i} \cup S^{B_i}) \setminus (S_r^{B_i} \cap S^{B_i}))$$

In the GIS context this non-negative metric appertains to commission and omission errors, and to false positives and false negatives: the union of the (i) subset that is estimated as shaded but in reality it is not with the (ii) subset of the inverse case.

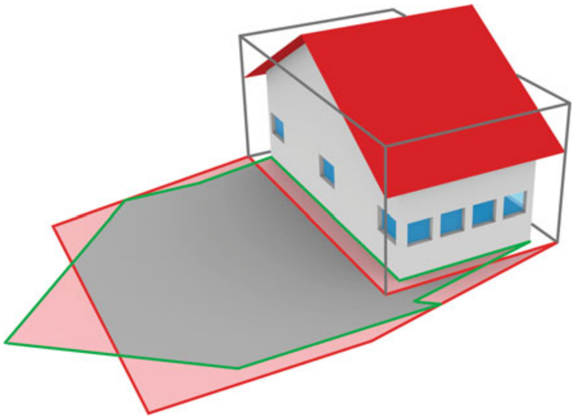

Fig. 4 A case of two shadows from an LOD1 and an LOD3 (outlined in *red* and *green*, respectively) that have the same area, showing that this error metric can be ambiguous. The area of their symmetric difference (*light red area*) is 28.7 m^2 (33.9 % in relative terms), and the Hausdorff distance in this case is 2.47 m

Because area is only one of the aspects that quantifies the extent of a shape, we compute the similarity between the two shapes, which is a fundamental subject in computer science and GIS (Arkin et al. 1991; Huttenlocher et al. 1993; Samal et al. 2004). There is a variety of methods and metrics to express the correspondence of two shapes in GIS (Ruiz et al. 2011; Goodchild and Hunter 1997), one of the prominent being the Hausdorff distance (Hausdorff 1914). It has been widely used in geoinformation science and 3D city modelling for diverse purposes (Min et al. 2007), for instance, to assess the quality of GIS data (Girres and Touya 2010), to assess the performance of 3D generalisation (Cignoni et al. 1998), to aid map matching (Mustiere and Devogele 2008), to analyse movement trajectories (Liu et al. 2012), and to detect changes between two CityGML models (Pédrinis et al. 2015).

The Hausdorff distance quantifies the mismatch between two geometries by identifying the point on one shape that is the maximum distance from the other shape, therefore we define the third shadow error metric as

$$\varepsilon_3^r = H(S_r^{B_i}, S^{B_i}) = \max(h(S_r^{B_i}, S^{B_i}), h(S^{B_i}, S_r^{B_i}))$$

where $h(A, B)$ is a function that finds the point $a \in A$ that is farthest from any point in B and measures the distance from a to its nearest neighbour in B:

$$h(A, B) = \max_{a \in A} \min_{b \in B} ||a - b||$$

For the three error metrics we compute their root-mean-square error (RMSE). While the Hausdorff distance technically is not an error, it is not uncommon to compute its root-mean-square value (Agarwal et al. 2010; Aspert et al. 2002).

For ε_1 and ε_2 we compute also the relative error (with respect to the true size of the shadow) to put the derived numbers in perspective, which is not possible for ε_3.

3.5 Implementation

Available implementations do not fully support our methodology. For instance, several GIS tools contain a module to forecast shadows at a specific timestamp, however, such functionality cannot be exploited to our advantage: the shadow cannot be exported as a vector geometry nor most of the tools can be automated. Furthermore, computer graphics software packages usually render a shadow only in raster format. Therefore, we have implemented in Python a software prototype that reads CityGML data, estimates their shadow for a particular location and timestamp, and exports it as a polygon.

The sun positions are taken from PyEphem/XEphem,[1] the implementation of the ephemeris of Bretagnon and Francou (1988). The shadow polygons operations (e.g. union and symmetric difference) are accomplished with Shapely.[2] The Hausdorff distance has been calculated with PostGIS.[3] For validating the correctness of shadows, we have first converted a CityGML model and its calculated polygon shadow to OBJ (with CityGML2OBJs; see Biljecki and Arroyo Ohori 2015), and imported it in Blender,[4] an open-source 3D computer graphics software. We have rendered the setting for the same date, time, and location, thanks to the Blender add-on Sun Position.[5] The shadows matched—this is evident in Fig. 3 where the rendered shaded area and the shadow polygon are conflated from independent workflows.

Some of the shadow polygons were found to include long tiny spikes due to floating point errors, which was inhibited with snap rounding (Hobby 1999), and triangulation-based polygon repair with the tool prepair (Ledoux et al. 2014).

In addition to calculating the error metrics, the computational cost was recorded (time and number of projected polygons), in order to suggest the load of each LOD.

4 Experiments

We have conducted experiments on 400 different buildings in 8 LODs ($400 \times 8 \times 81 = 259$k shadows in total). We present the errors in Fig. 5 and Table 1, and discuss them in Sect. 4.1.

[1]https://pypi.python.org/pypi/pyephem/ and http://www.clearskyinstitute.com/xephem/.

[2]https://pypi.python.org/pypi/Shapely.

[3]http://postgis.net.

[4]https://www.blender.org.

[5]http://wiki.blender.org/index.php/Extensions:2.6/Py/Scripts/3D_interaction/Sun_Position.

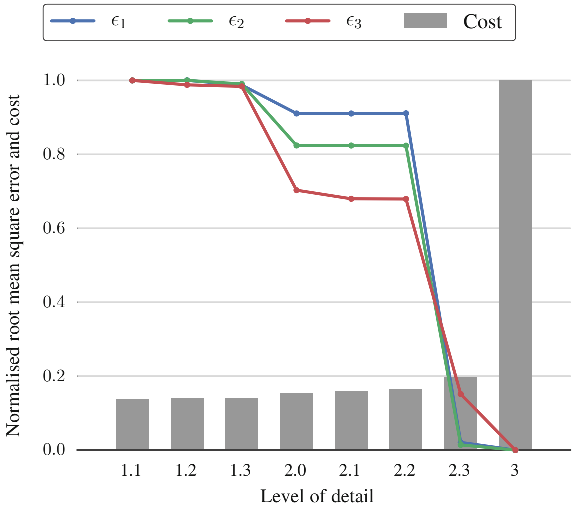

Fig. 5 Errors and computation cost for each LOD. The metrics are normalised according to the least favourable result

Table 1 Numerical results of the experiments. The error metrics are expressed as RMS values

LOD	ε_1		ε_2		ε_3
	(m^2)	(%)	(m^2)	(%)	(m)
1.1	27.6	16.2	40.3	30.1	2.5
1.2	27.6	16.2	40.3	30.1	2.4
1.3	27.2	16.0	39.9	29.9	2.4
2.0	25.1	13.1	33.3	20.7	1.8
2.1	25.1	13.1	33.3	20.7	1.6
2.2	25.1	13.1	33.2	20.6	1.6
2.3	0.5	0.7	0.5	0.7	0.4

4.1 *Findings and Discussion*

The main findings of the experiments, as shown in Fig. 5 and Table 1, suggest that the relative errors between most LODs are small, and the improvements of each LOD are not significant. Furthermore, we point out other findings:

- The improvement of LOD2 over LOD1 is almost negligible if considering the shadow as a whole (only a 3 % reduction in the area error).
- Overall, a finer LOD does bring a more accurate result. However, that is not always the case for each building. The improvement depends on the configuration of the analysed area. As an example, Fig. 7 shows the distribution of $\varepsilon_2, \varepsilon_3$ errors for LOD 2.2. It shows that for many buildings the error is negligible (e.g. in that LOD

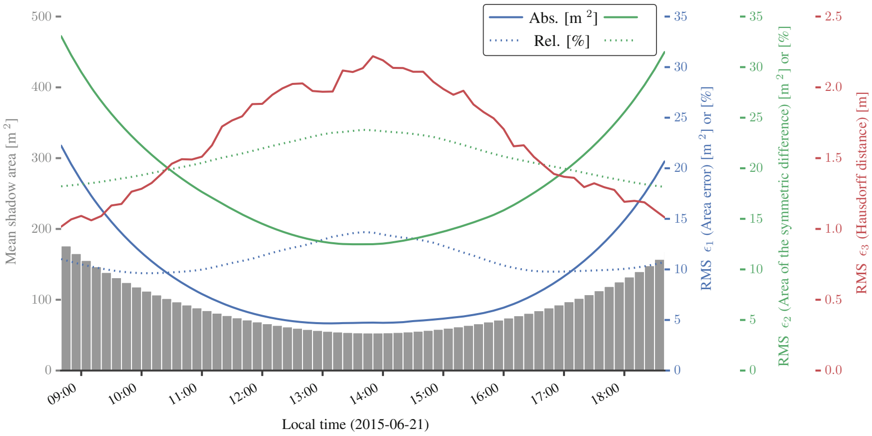

Fig. 6 This combined plot shows the variable behaviour of the three error metrics with respect to the position of the sun, and thus—the size of the shadow in the ground. The values refer to LOD2.2

for 19 % buildings there is no error ε_2; for LOD1.1 that value is at 10 %). A more detailed inspection revealed that this applies to buildings with flat roofs and no roof superstructures. If such buildings dominate in an area to be analysed, the acquisition of finer LODs is probably not beneficial.

- Modelling dormers (LOD2.2 and 2.3) and other roof details has a negligible influence on the quality of the prediction. This can be explained by the fact that dormers and chimneys are not present in all buildings, and they make a difference only during a limited time of the day (see the example in Fig. 2).
- Different data (types of buildings) and different settings (day, time, location) result in a different behaviour and magnitude of the error, indicating that related experiments should be diverse. Figure 6 shows the variation of the magnitude of errors as a function of time during one day.
- Figure 6 also shows that while in absolute terms the ε_1 and ε_2 errors increase with the actual size of the shadow (close to sunrise and sunset), their relative counterparts decrease. Furthermore, the behaviour of ε_3 is different.
- LOD3 contains openings, which have no influence on the shadows (unless in the special case of the sun rays passing through two windows, but this triviality was not taken into account). The improvement over LOD2 is mostly caused by overhangs and other smaller details, which on the other hand are probably not appreciated by the use cases that require shadow estimation as an input. Furthermore, an LOD3 model entails a substantial cost of acquisition and processing, which also has to be taken into account.

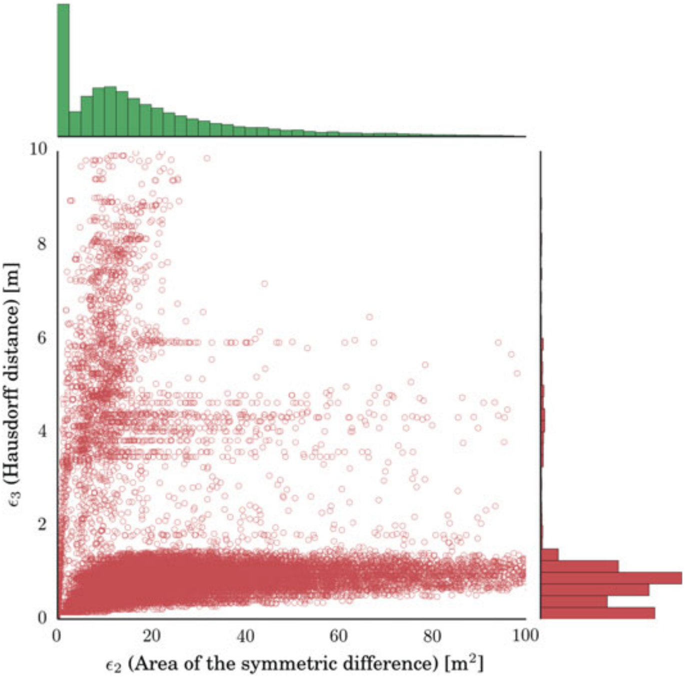

Fig. 7 Scatter plot showing the relation between the error metrics $\varepsilon_2, \varepsilon_3$ and their distribution (for LOD2.2). The histogram on the *right* shows the distribution of ε_3, while the one on *top* shows the distribution of ε_2. The latter shows that for a substantial share of samples the error ε_2 is insignificant

4.2 Evaluation of Error Metrics

The results of a seemingly simple analysis of determining the accuracy of a shadow estimation show that errors can be approached from different perspectives. Figure 7 shows the relation between our second and third error metrics, and the distribution for each. We have computed the correlation between the errors to investigate their relation:

$$r_{|\varepsilon_1|,\varepsilon_2} = 0.967 \qquad r_{|\varepsilon_1|,\varepsilon_3} = 0.099 \qquad r_{\varepsilon_2,\varepsilon_3} = 0.085$$

An interesting outcome is that there is a low degree of correlation between the area error metrics and the Hausdorff distance. As visible in the scatter plot, there are several cases in which the magnitude of the area error metrics (ε_1 and ε_2) are small (<0.1 m^2), with a significant value of ε_3. This is most evident in the results of LOD2.3 where the first two error metrics are low, and the Hausdorff distance is not negligible. Manual inspection revealed that these deviations are caused by small LOD3-only details such as chimneys, which render small shadow area differences, but since they protrude, ε_3 is of noticeable value (e.g. see the chimney in Fig. 3).

We are ambivalent on the use of the Hausdorff distance for this purpose. Besides the advantage that ε_3 revealed some discrepancies that were not detected by the first two, it helped to put the area errors in perspective, i.e. some large area errors were in fact caused by practically insignificant deviations (e.g. long and narrow strips of shadows). The disadvantage is that the Hausdorff distance is not a stable error metric (see Fig. 6), and it is sensitive to computational and geometric errors, e.g. caused by floating point errors and slivers.

For the first two error metrics we have computed also a relative counterpart, as the relation to the total size of the shadow. This helped to understand the true magnitude of the error (e.g. that the RMS of ε_2 for LOD1.2 is 16 % of the shadow size).

5 Conclusions

In this paper we have presented a study on the influence of the LOD of a 3D building model on the quality on a 3D GIS spatial analysis. We benchmark the accuracy of 8 LODs for estimating the shadow, and conclude that investing in a data set with a fine LOD is not always a good idea. For instance, for 50 % of buildings modelled in the coarse LOD1.1, the error (ε_1) is within 10.2 % of the size of the shadow (percentile rank of a score), which practically does not have much influence for some use cases. For areas with a higher share of buildings with a flat roof this fact would be even more substantiated.

Therefore, we refute the universally accepted assumption that finer LODs inherently bring more accurate results in spatial analyses, and we argue that such analyses should be conducted to understand the impact of LOD on a specific use case.

Shadows do not have a unique metric, a fact that is also valid for many other spatial analyses. We use three error metrics: area error (ε_1), area of the symmetric difference (ε_2), and the Hausdorff distance (ε_3), which show different observations. In our study, we determine the influence of the resolution of the models on raw shadows as standalone concepts. While we find that the LOD has a variable influence, these smaller improvements may not always benefit a use case. Actually, it may damage it: while the improvement is negligible, the acquisition and processing costs could be substantially higher. This depends on the *weight* a shadow has as an input in a use case. For instance, in geo-visualisation a more accurate shadow probably does not make any difference, while in some other such as predicting the yield of photovoltaic panels it might be tangible.

For future work we plan to investigate the significance and influence of the LOD on the outcome of a use case that uses estimated shadows as input. For instance, the error in the prediction of the duration a wall is shaded during the day, or the error in the estimation of the loss of the solar potential in kWh/year due to shadows.

Furthermore, we plan to investigate the benchmarking of continuous LODs (Arroyo Ohori et al. 2015).

Acknowledgments The detailed observations raised during the peer-review are gratefully acknowledged. We are thankful to the developers of the open-source software that was used in the realisation of this work, and to Ken Arroyo Ohori for suggestions which have accelerated the development of the method. This research is supported by the Dutch Technology Foundation STW, which is part of the Netherlands Organisation for Scientific Research (NWO), and which is partly funded by the Ministry of Economic Affairs (project code: 11300).

References

Agarwal, P. K., Har-Peled, S., Sharir, M., & Wang, Y. (2010). Hausdorff distance under translation for points and balls. *ACM Transactions on Algorithms*, *6*(4), 1–26. Aug.

Alam, N., Coors, V., & Zlatanova, S. (2013). Detecting shadow for direct radiation using CityGML models for photovoltaic potentiality analysis. In C. Ellul, S. Zlatanova, M. Rumor, & R. Laurini (Eds.), *Urban and regional data management* (pp. 191–196). London, UK: CRC Press.

Appleton, K., & Lovett, A. (2003). GIS-based visualisation of rural landscapes: defining 'sufficient' realism for environmental decision-making. *Landscape and Urban Planning*, *65*(3), 117–131.

Arkin, E. M., Chew, L. P., Huttenlocher, D. P., Kedem, K., & Mitchell, J. S. B. (1991). An efficiently computable metric for comparing polygonal shapes. *IEEE Transactions on Pattern Analysis and Machine Intelligence*, *13*(3), 209–216. Mar.

Arroyo Ohori, K., Ledoux, H., Biljecki, F., & Stoter, J. (2015). Modeling a 3D city model and its levels of detail as a true 4D model. *ISPRS International Journal of Geo-Information*, *4*(3), 1055–1075.

Aspert, N., Santa-Cruz, D., & Ebrahimi, T. (2002). MESH: measuring errors between surfaces using the Hausdorff distance. In *IEEE international conference on multimedia and expo (ICME)* (pp. 705–708). IEEE.

Bartie, P., Reitsma, F., Kingham, S., & Mills, S. (2010). Advancing visibility modelling algorithms for urban environments. *Computers, Environment and Urban Systems*, *34*(6), 518–531. Nov.

Besuievsky, G., Barroso, S., Beckers, B., & Patow, G. (2014). A configurable LoD for procedural urban models intended for daylight simulation. In G. Besuievsky & V. Tourre (Eds.), *Proceedings of the eurographics workshop on urban data modelling and visualisation* (pp. 19–24). Strasbourg, France: The Eurographics Association. Apr.

Biljecki, F., & Arroyo Ohori, K. (2015). Automatic semantic-preserving conversion between OBJ and CityGML. In *Eurographics workshop on urban data modelling and visualisation 2015* (pp. 25–30), Delft, Netherlands.

Biljecki, F., Ledoux, H., & Stoter, J. (2014a). Error propagation in the computation of volumes in 3D city models with the Monte Carlo method. *ISPRS annals photogrammetry, remote sensing and spatial information sciences*, *II*(2), 31–39.

Biljecki, F., Ledoux, H., Stoter, J., & Zhao, J. (2014b). Formalisation of the level of detail in 3D city modelling. *Computers, Environment and Urban Systems*, *48*, 1–15. Nov.

Biljecki, F., Heuvelink, G. B. M., Ledoux, H., & Stoter, J. (2015a). Propagation of positional error in 3D GIS: estimation of the solar irradiation of building roofs. *International Journal of Geographical Information Science*, *29*(12), 2269–2294. Dec.

Biljecki, F., Ledoux, H., & Stoter, J. (2015b). Improving the consistency of multi-LOD CityGML datasets by removing redundancy. In M. Breunig, A.-D. Mulhim, E. Butwilowski, P. V. Kuper, J. Benner, & K.-H. Häfele (Eds.), *3D geoinformation science* (pp. 1–17). Springer.

Biljecki, F., Stoter, J., Ledoux, H., Zlatanova, S., & Çöltekin, A. (2015c). Applications of 3D city models: State of the art review. *ISPRS International Journal of Geo-Information*, *4*(4), 2842–2889. Dec. http://doi.org/10.3390/ijgi4042842.

Biljecki, F., Ledoux, H., & Stoter, J. (2016). An improved LOD specification for 3D building models. *Computers, Environment and Urban Systems*, *59*, 25–37.

Blinn, J. (1988). Me and my (fake) shadow. *IEEE Computer Graphics and Applications*, *8*(1), 82–86. Jan.

Boeters, R., Arroyo Ohori, K., F., Biljecki, & S. Zlatanova. (2015). Automatically enhancing CityGML LOD2 models with a corresponding indoor geometry. *International Journal of Geographical Information Science*, *29*(12), 2248–2268.

Booij, M. J. (2005). Impact of climate change on river flooding assessed with different spatial model resolutions. *Journal of Hydrology*, *303*(1–4), 176–198. Mar.

Brasebin, M., Perret, J., Mustière, S., & Weber, C. (2012). Measuring the impact of 3D data geometric modeling on spatial analysis: illustration with Skyview factor. In T. Leduc, G. Moreau, & R. Billen (Eds.), *Usage, usability, and utility of 3D city models—European COST action TU0801* (pp. (02001)1–16), Nantes, France, Oct. 2012. EDP Sciences.

Bretagnon, P., & Francou, G. (1988). Planetary theories in rectangular and spherical variables. VSOP 87 solutions. *Astronomy and Astrophysics*, *202*, 309–315. Aug.

Burnicki, A. C., Brown, D. G., & Goovaerts, P. (2007). Simulating error propagation in land-cover change analysis: The implications of temporal dependence. *Computers, Environment and Urban Systems*, *31*(3), 282–302. May.

Carneiro, C., & Golay, F. (2009). Solar radiation over the urban texture: LIDAR data and image processing techniques for environmental analysis at city scale. In J. Lee & S. Zlatanova (Eds.), *3D Geo-Information Sciences* (pp. 319–340). Heidelberg: Springer.

Chaubey, I., Cotter, A. S., Costello, T. A., & Soerens, T. S. (2005). Effect of DEM data resolution on SWAT output uncertainty. *Hydrological Processes*, *19*(3), 621–628. Feb.

Cignoni, P., Rocchini, C., & Scopigno, R. (1998). Metro: Measuring error on simplified surfaces. *Computer Graphics Forum*, *17*(2), 167–174. June.

City of Mississauga. Standards for shadow studies, Feb. 2012. http://www6.mississauga.ca/onlinemaps/planbldg/UrbanDesign/ShadowStudiesFinal_Feb2012.pdf.

Den Haag (2011). Voorstel van het college inzake beleid dakopbouwen. *RIS*, *180461*.

Eicker, U., Monien, D., Duminil, E., & Nouvel, R. (2015). Energy performance assessment in urban planning competitions. *Applied Energy*, *155*, 323–333. Oct.

Girres, J.-F., & Touya, G. (2010). Quality assessment of the French openstreetmap dataset. *Transactions in GIS*, *14*(4), 435–459.

Goodchild, M. F., & Hunter, G. J. (1997). A simple positional accuracy measure for linear features. *International Journal of Geographical Information Science*, *11*(3), 299–306. Apr.

Gröger, G., & Plümer, L. (2012). CityGML—interoperable semantic 3D city models. *ISPRS Journal of Photogrammetry and Remote Sensing*, *71*, 12–33. July.

Hausdorff, F. (1914). *Grundzüge der Mengenlehre*. Leipzig, Germany: Verlag von Veit and Comp.

Helbich, M., Jochem, A., Mücke, W., & Höfle, B. (2013). Boosting the predictive accuracy of urban hedonic house price models through airborne laser scanning. *Computers, Environment and Urban Systems*, *39*(C), 81–92.

Hengl, T. (2006). Finding the right pixel size. *Computers and Geosciences*, *32*(9), 1283–1298. Nov.

Herbert, G., & Chen, X. (2015). A comparison of usefulness of 2D and 3D representations of urban planning. *Cartography and Geographic Information Science*, *42*(1), 22–32.

Hobby, J. D. (1999). Practical segment intersection with finite precision output. *Computational Geometry*, *13*(4), 199–214. Oct.

Hofierka, J., & Zlocha, M. (2012). A new 3-D solar radiation model for 3-D city models. *Transactions in GIS*, *16*(5), 681–690. Oct.

Huttenlocher, D. P., Klanderman, G. A., & Rucklidge, W. J. (1993). Comparing images using the Hausdorff distance. *IEEE Transactions on Pattern Analysis and Machine Intelligence*, *15*(9), 850–863. Sept.

Hwang, R.-L., Lin, T.-P., & Matzarakis, A. (2011). Seasonal effects of urban street shading on long-term outdoor thermal comfort. *Building and Environment*, *46*(4), 863–870. Apr.

Jochem, A., Höfle, B., Rutzinger, M., & Pfeifer, N. (2009). Automatic roof plane detection and analysis in airborne lidar point clouds for solar potential assessment. *Sensors*, *9*(7), 5241–5262. July.

Kibria, M. S., Zlatanova, S., Itard, L., & Dorst, M. (2009). GeoVEs as tools to communicate in urban projects: requirements for functionality and visualization. In *3D geo-information sciences* (pp. 379–395). Heidelberg: Springer.

Knowles, R. L. (2003). The solar envelope: Its meaning for energy and buildings. *Energy and Buildings*, *35*(1), 15–25. Jan.

Kumar, L., Skidmore, A. K., & Knowles, E. (1997). Modelling topographic variation in solar radiation in a GIS environment. *International Journal of Geographical Information Science*, *11*(5), 475–497. July.

Lange, E., & Hehl-Lange, S. (2005). Combining a participatory planning approach with a virtual landscape model for the siting of wind turbines. *Journal of Environmental Planning and Management*, *48*(6), 833–852. Nov.

Ledoux, H., Arroyo Ohori, K., & M. Meijers. (2014). A triangulation-based approach to automatically repair GIS polygons. *Computers and Geosciences*, *66*, 121–131.

Li, Y., Brimicombe, A. J., & Ralphs, M. P. (2000). Spatial data quality and sensitivity analysis in GIS and environmental modelling: the case of coastal oil spills. *Computers, Environment and Urban Systems*, *24*(2), 95–108. Mar.

Ling, Y., Ehlers, M., Usery, E. L., & Madden, M. (2008). Effects of spatial resolution ratio in image fusion. *International Journal of Remote Sensing*, *29*(7), 2157–2167. Apr.

Liu, L., Qiao, S., Zhang, Y., & Hu, J. (2012). An efficient outlying trajectories mining approach based on relative distance. *International Journal of Geographical Information Science*, *26*(10), 1789–1810. Oct.

Luebke, D., Reddy, M., Cohen, J. D., Varshney, A., Watson, B., & Huebner, R. (2003). *Level of detail for 3D graphics*. Morgan Kaufmann Pub.

Mardaljevic, J., & Rylatt, M. (2003). Irradiation mapping of complex urban environments: an image-based approach. *Energy and Buildings*, *35*(1), 27–35. Jan.

Min, D., Zhilin, L., & Xiaoyong, C. (2007). Extended Hausdorff distance for spatial objects in GIS. *International Journal of Geographical Information Science*, *21*(4), 459–475. Apr.

Möller, T., & Trumbore, B. (1997). Fast, minimum storage ray-triangle intersection. *Journal of Graphics Tools*, *2*(1), 21–28.

Morello, E., & Ratti, C. (2009). Sunscapes: 'Solar envelopes' and the analysis of urban DEMs. *Computers, Environment and Urban Systems*, *33*(1), 26–34.

Mustiere, S., & Devogele, T. (2008). Matching networks with different levels of detail. *GeoInformatica*, *12*(4), 435–453.

Nguyen, H. T., & Pearce, J. M. (2012). Incorporating shading losses in solar photovoltaic potential assessment at the municipal scale. *Solar Energy*, *86*(5), 1245–1260. May.

Pédrinis, F., Morel, M., & Gesquière, G. (2015). Change detection of cities. In *3D geoinformation science* (pp. 123–139). Springer.

Peters, R., Ledoux, H., & Biljecki, F. (2015). Visibility analysis in a point cloud based on the medial axis transform. In *Eurographics workshop on urban data modelling and visualisation 2015* (pp. 7–12), Delft, Netherlands.

Pogson, M., & Smith, P. (2015). Effect of spatial data resolution on uncertainty. *Environmental Modelling and Software*, *63*, 87–96. Jan.

Redweik, P., Catita, C., Brito, M., & Brito, M. (2013). Solar energy potential on roofs and facades in an urban landscape. *Solar Energy*, *97*, 332–341. Nov.

Ruiz, J. J., Ariza, F. J., Ureña, M. A., & Blázquez, E. B. (2011). Digital map conflation: a review of the process and a proposal for classification. *International Journal of Geographical Information Science*, *25*(9), 1439–1466. Sept.

Samal, A., Seth, S., & Cueto, K. (2004). A feature-based approach to conflation of geospatial sources. *International Journal of Geographical Information Science*, *18*(5), 459–489. July.

Stoter, J., de Kluijver, H., & Kurakula, V. (2008). 3D noise mapping in urban areas. *International Journal of Geographical Information Science*, *22*(8), 907–924. Aug.

Strzalka, A., Bogdahn, J., Coors, V., & Eicker, U. (2011). 3D city modeling for urban scale heating energy demand forecasting. *HVAC&R Research*, *17*(4), 526–539.

Strzalka, A., Alam, N., Duminil, E., Coors, V., & Eicker, U. (2012). Large scale integration of photovoltaics in cities. *Applied Energy*, *93*, 413–421. May.

Tooke, T. R., Coops, N. C., Voogt, J. A., & Meitner, M. J. (2011). Tree structure influences on rooftop-received solar radiation. *Landscape and Urban Planning*, *102*(2), 73–81. Aug.

Usery, E. L., Finn, M. P., Scheidt, D. J., Ruhl, S., Beard, T., & Bearden, M. (2004). Geospatial data resampling and resolution effects on watershed modeling: A case study using the agricultural non-point source pollution model. *Journal of Geographical Systems*, *6*(3), 289–306. Oct.

Whitted, T. (1980). An improved illumination model for shaded display. *Communications of the ACM*, *23*(6), 343–349. June.

Williams, L. (1978). Casting curved shadows on curved surfaces. *ACM SIGGRAPH Computer Graphics*, *12*(3), 270–274. Aug.

Woo, A., Poulin, P., & Fournier, A. (1990). A survey of shadow algorithms. *IEEE Computer Graphics and Applications*, *10*(6), 13–32.

Yezioro, A., & Shaviv, E. (1994). Shading: A design tool for analyzing mutual shading between buildings. *Solar Energy*, *52*(1), 27–37. Jan.

http://www.springer.com/978-3-319-25689-4

Advances in 3D Geoinformation
Abdul-Rahman, A. (Ed.)
2017, VII, 512 p. 266 illus., 204 illus. in color.,
Hardcover
ISBN: 978-3-319-25689-4